

# Photocatalytic oxidation of benzyl alcohols by three-dimensional reduced graphene oxide/nano zinc oxide catalyst under visible light

Yuxiang Wang<sup>a</sup>, Xianlong Zhang<sup>a</sup>, Lihua Wang<sup>b</sup> and Youjian Chen<sup>a\*</sup>

<sup>a</sup>College of Chemistry and Materials Engineering, Wenzhou University, Wenzhou, Zhejiang 325027, P.R. China

<sup>b</sup>Shimadzu (China) Co., Ltd. Guangzhou, Guangdong 510140, P.R. China

A three-dimensional reduced graphene oxide/nano zinc oxide (3D-RGO/ZnO) composite photocatalyst has been prepared through an *in situ* reduction of GO and growth of nano ZnO particles process. The 3D-RGO/ZnO catalyst displayed enhanced photocatalytic activity towards commercial ZnO nanoparticles and can be applied to the oxidation of a broad series of benzyl alcohols including primary and secondary alcohols to corresponding carbonyl compounds under the irradiation of visible light. A plausible photocatalytic mechanism referring to photo electron generation and transfer has been proposed.

**Keywords:** reduced graphene, zinc oxide, photocatalysis, oxidation, primary and secondary alcohols

One of the most fundamental approaches to synthesise carbonyl compounds is the oxidation of alcohols *via* commonly used inorganic oxidants such as  $(\text{NH}_4)_2\text{Ce}(\text{NO}_3)_6$ ,<sup>1</sup>  $\text{CrO}_3$ ,<sup>2</sup> Corey–Suggs reagent<sup>3</sup> and  $\text{MnO}_2$ ,<sup>4</sup> and organic oxidants such as 9-azabicyclo[3.3.1]nonane *N*-oxyl (ABNO),<sup>5</sup> 2-azaadamantane *N*-oxyl (AZADO),<sup>6</sup> 2,2,6,6-tetramethylpiperidinyloxy (TEMPO)<sup>7</sup> and 2-iodoxybenzoic acid (IBX).<sup>8,9</sup> However, most existing oxidants have problems including high toxicities, difficult recovery and dangerous operation which limited their broad applications. As a clean, abundant, and sustainable energy source, efficient utilisation of solar energy is of great importance.<sup>10</sup> If we can effectively use solar energy to achieve the hydroxyl–carbonyl transformation, traditional inorganic and organic oxidants may not be indispensable. The crucial factor is to prepare an appropriate photocatalyst. To date, many photocatalysts have been developed, such as Mott–Schottky heterojunctions,<sup>11</sup> Au–Pd alloy,<sup>12–14</sup> and Pd nanostructures,<sup>15,16</sup> for photocatalytic organic reactions, as well as semiconductors for photocatalytic degradation of pollutants.<sup>17,18</sup> Compared to noble metal catalysts, inexpensive semiconductors with a wide-band gap have competitive potential. Under the irradiation of light, efficient photogeneration and transfer of electron can take place at the interfaces of semiconductor to organic reactants, thus displaying excellent photocatalytic effects. For example, titanium dioxide ( $\text{TiO}_2$ ) can effectively catalyse the oxidation of benzyl alcohols into corresponding aldehydes under visible light irradiation.<sup>19</sup> Zinc oxide ( $\text{ZnO}$ ) which, like  $\text{TiO}_2$ , is a common wide bandgap semiconductor, has many applications in the fields of electroluminescence,<sup>20</sup> photodetector,<sup>21</sup> dye degradation,<sup>22</sup> and photocatalysis.<sup>23,24</sup>  $\text{ZnO}$  possesses excellent optical activities and light-energy transformations, implying it has a great potential for the photocatalytic oxidation of benzyl alcohols.

Three-dimensional reduced graphene oxide (3D-RGO), a kind of two-dimensional (2D) carbon material, usually prepared from graphene oxide (GO) through thermal,<sup>25</sup> chemical,<sup>26</sup> and hydrothermal<sup>27</sup> processes has shown great potential in a broad range of applications, such as polymer composites,<sup>28,29</sup> chemical and biological sensors,<sup>30</sup> energy-storage,<sup>31</sup> electrocatalysis,<sup>32</sup> and environmental disposal.<sup>33</sup> Due to their high specific surface area and OH groups, many nanoparticles can be deposited on the surface of RGO through a *in situ* growth process, and thus 3D-RGO/nanoparticles composites form which can display enhanced performances toward single nanoparticles including electromagnetic absorption,<sup>34</sup> and photoelectric conversion.<sup>35</sup>

To combine the outstanding performances of 3D-RGO and nano  $\text{ZnO}$ , we first synthesised a 3D-RGO/ $\text{ZnO}$  composite photocatalyst through an *in situ* reduction of GO and growth of nano  $\text{ZnO}$  particles and then applied this photocatalyst to the photocatalytic oxidation of benzyl alcohols.

## Experimental

All reagents were purchased from commercial companies without purification. Distilled water was obtained from Direct-Q3 UV, Millipore.

### *Synthesis and purification of graphene oxide*

Graphite oxide was prepared by a modified Hummers method. In brief, concentrated  $\text{H}_2\text{SO}_4$  (50 mL) was added to graphite (1.0 g) under an ice bath and stirred for 3 h. Then,  $\text{KMnO}_4$  (4.0 g) was slowly added. After stirring for 2 h, distilled water (100 mL) was added dropwise. After additional stirring for 30 min,  $\text{H}_2\text{O}_2$  (10 mL) was slowly added to this solution and bright yellow graphite oxide appeared. The graphite oxide was filtered and washed four times with distilled water and freeze-dried at  $-50\text{ }^\circ\text{C}$  for 24 h to obtain graphite oxide powder. The graphite oxide powder was dispersed in distilled water as  $1\text{ mg mL}^{-1}$ , ultrasonicated for 30 min, and centrifuged at  $10,000\text{ rev min}^{-1}$  for 30 min to obtain GO as the supernatant. This was freeze-dried at  $-50\text{ }^\circ\text{C}$  to furnish the GO sponge.

### *Synthesis of 3D-RGO/ $\text{ZnO}$ photocatalyst*

GO sponge (120 mg) was dispersed in distilled water (40 mL) by sonification for 30 min to form solution A. Anhydrous  $\text{Zn}(\text{OAc})_2$  (120 mg) was dissolved in ethanol (80 mL) to form solution B. Ethylenediamine (0.5 mL) was added to the mixture of solution A and B, and the resultant mixture was sealed in a 200-mL Teflon-lined autoclave and maintained at  $180\text{ }^\circ\text{C}$  for 12 h. Then the autoclave was naturally cooled to room temperature and the as-prepared 3D-RGO/ $\text{ZnO}$  was washed with distilled water and freeze-dried to obtain the 3D-RGO/ $\text{ZnO}$  photocatalyst.

### *Photocatalytic oxidation of benzyl alcohols by 3D-RGO/ $\text{ZnO}$ photocatalyst*

A 25 mL round-bottomed flask was charged with alcohol (1 mmol), 3D-RGO/ $\text{ZnO}$  (40 mg) and *N,N*-dimethyl formamide (5 mL). The resultant mixture was stirred under  $\text{O}_2$  with two white LED lamps (12 W). After completion of the reaction, the 3D-RGO/ $\text{ZnO}$  catalyst was recycled by filtration and the organic phase of the filtrate was extracted with  $\text{EtOAc}$ , washed three times with water and dried over  $\text{Na}_2\text{SO}_4$ . The pure product was then isolated by silica chromatography using petroleum ether/ $\text{EtOAc}$  mixtures as the eluent.

\* Correspondent. E-mail: chenyoujian1985@163.com

### Characterisation of catalyst and oxidation products

The detailed morphologies of the 3D-RGO/ZnO were observed with a field emission scanning electron microscope (FE-SEM, S4800, Hitachi) and field emission high resolution transmission electron microscope (FE-HRTEM, Tecnai G2 F30 S, FEI). The crystal structure of the as-synthesised 3D-RGO/ZnO was identified by X-ray diffractometer (XRD, X' Pert Pro, Philips), using Cu K $\alpha$  ( $\lambda = 1.54 \text{ \AA}$ ) radiation. X-ray photoelectron spectra (XPS) was carried out in a Thermo Scientific ESCALAB 250Xi X-ray photoelectron spectrometer equipped with a monochromatic Al K X-ray source (1486.6 eV). NMR spectra were obtained with a Bruker Avance 500 spectrometer or Bruker Avance 300 spectrometer.

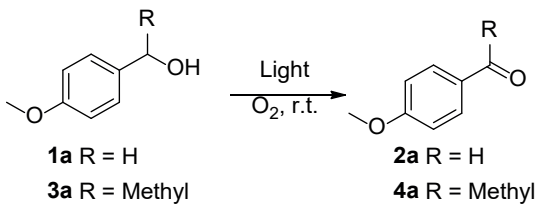
### Results and discussion

GO nanosheets were self-assembled to form a 3D structure and reduced to RGO under hydrothermal conditions. Meanwhile, ZnO nanoparticles were supported on 3D-RGO sheets through an *in situ* growth process and dispersed evenly in the interconnected 3D porous network (Fig. 1a). TEM was used to investigate the crystal size as well as morphology of ZnO nanoparticles. Figure 1b shows that ZnO nanoparticles with a size less than 500 nm are symmetrically attached to the surface of RGO without disassociated ZnO. In Fig. 1c, the broad diffraction peak of graphite (002) implied sufficient removal of oxygen functional groups from the surface of GO.<sup>36</sup> The strong and sharp peaks at  $2\theta = 31.61, 34.50, 36.33, 47.57, 56.59^\circ$  were consistent with the standard XRD data for the (100), (002), (101), (102) and (110) planes of ZnO. Figure 1d shows the XPS spectrum of 3D-RGO/ZnO photocatalyst. Except for the apparent C1s and O1s peaks, the Zn2p peak is very weak in the XPS spectrum, which may be attributed to the low content of the ZnO in the catalyst.

To examine the photocatalytic activity of 3D-RGO/ZnO catalyst, (4-methoxyphenyl)methanol (**1a**) and 1-(4-methoxyphenyl) ethanol (**3a**) were used as model compounds and the results are summarised in Table 1. Trace of oxidation product (**2a**) can be obtained without using light (Table 1, entry 1). But the oxidation of alcohol (**1a**) proceeded smoothly to furnish corresponding aldehyde (**2a**) in excellent yields under irradiation of UV light as well as visible (Vis) light (Table 1, entries 2 and 3). We next explored the activity of 3D-RGO/ZnO catalyst under visible light because this

is much more convenient than using UV light. Obviously, no reaction took place without a 3D-RGO/ZnO catalyst even with enhanced visible light (Table 1, entry 4). Commercial nano ZnO particles can promote the oxidation reaction to furnish desirable aldehyde in good yield (Table 1, entry 5), but not so effectively as 3D-RGO/ZnO, indicating an enhanced catalytic effect when using 3D-RGO. 3D-RGO should play a role in acceleration of the reaction but cannot catalyse the reaction (Table 1, entry 6). The solvents can influence the oxidation efficiencies of **1a**. Apart from dimethylformamide (DMF), other solvents such as tetrahydrofuran (THF), acetone, ethyl acetate (EtOAc), and dimethyl sulfoxide (DMSO) have been also examined

**Table 1** Optimising conditions for the oxidation of alcohols<sup>a</sup>



Entry	Catalyst	Light	Solvent	Yield /% <sup>b</sup>
1	3D-RGO/ZnO	None	DMF	Trace
2	3D-RGO/ZnO	UV	DMF	91
3	3D-RGO/ZnO	Vis	DMF	96
4	3D-RGO/ZnO	Vis	DMF	0 <sup>c</sup>
5	Nano ZnO	Vis	DMF	85
6	3D-RGO	Vis	DMF	0
7	3D-RGO/ZnO	Vis	THF	82
8	3D-RGO/ZnO	Vis	Acetone	76
9	3D-RGO/ZnO	Vis	EtOAc	78
10	3D-RGO/ZnO	Vis	DMSO	87
11	3D-RGO/ZnO	Vis	DMF	93 <sup>d</sup>

<sup>a</sup> Reaction conditions: (4-methoxyphenyl) methanol **1a** (1 mmol), 3D-RGO/ZnO catalyst (40 mg), solvent (5 mL), O<sub>2</sub> atmosphere, room temperature, 6 h.

<sup>b</sup> Isolated yield.

<sup>c</sup> Without 3D-RGO/ZnO.

<sup>d</sup> 1-(4-Methoxyphenyl) ethanol **3a** (1 mmol) was used instead of (4-methoxyphenyl) methanol.

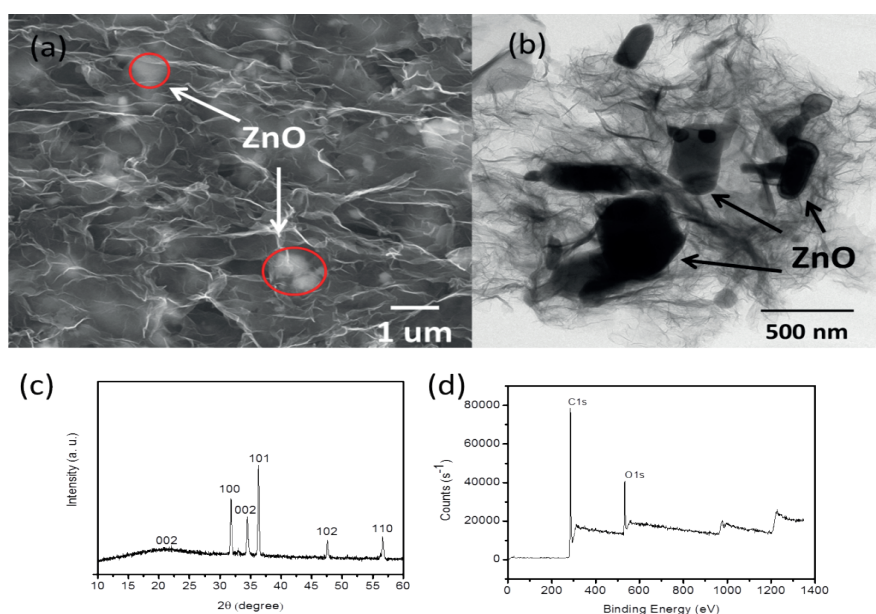
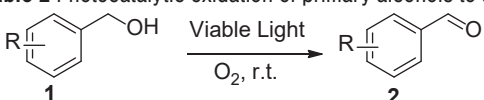


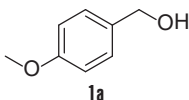
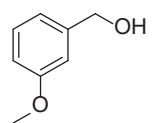
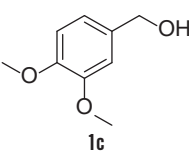
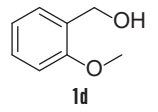
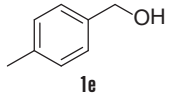
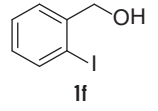
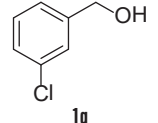
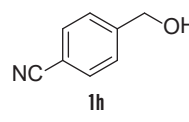
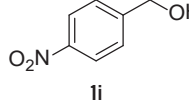
**Fig. 1** (a) SEM image, (b) TEM image, (c) XRD pattern, and (d) XPS spectrum of 3D-RGO/ZnO catalyst.

for the photocatalytic oxidation reaction, but lower yields of target product were obtained (Table 1, entries 7–10). Under the optimised condition, 1-(4-methoxyphenyl) ethanol **3a** can also be oxidised to ketone, implying an application for the oxidation of secondary alcohols (Table 1, entry 11).

Under optimised conditions, a series of primary alcohols have been used as substrates to explore the scope of 3D-RGO/ZnO photocatalysed oxidation. As shown in Table 2, the aryl alcohols which bear electron-donating groups can be smoothly oxidised to the corresponding aldehydes in high yields (Table 2, entries 1–5). When the halogen was introduced into the structure of substrates, the yields of products **2f** and **2g** decreased slightly (Table 2, entries 6 and 7). The oxidation reactions were seriously suppressed with the existence of strong electron-withdrawing groups such as  $-\text{CN}$ , and  $-\text{NO}_2$ . The above results show that

**Table 2** Photocatalytic oxidation of primary alcohols to aldehydes<sup>a</sup>



Entry	Substrate	Product	Yield /% <sup>b</sup>
1		<b>2a</b>	96
2		<b>2b</b>	92
3		<b>2c</b>	94
4		<b>2d</b>	91
5		<b>2e</b>	95
6		<b>2f</b>	88
7		<b>2g</b>	81
8		<b>2h</b>	76
9		<b>2i</b>	64

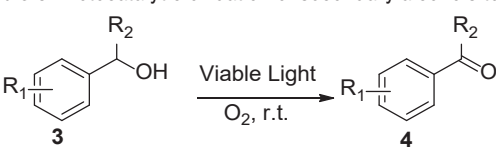
<sup>a</sup> Reaction conditions: primary alcohol **1** (1 mmol), 3D-RGO/ZnO catalyst (40 mg), DMF (5 mL), O<sub>2</sub> atmosphere, room temperature, 6 h.

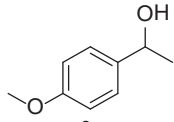
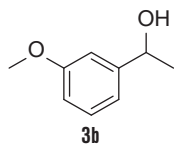
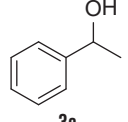
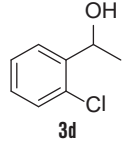
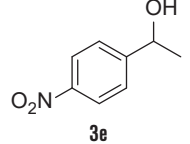
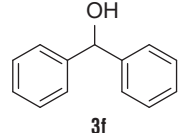
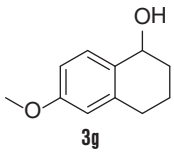
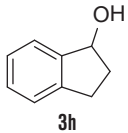
<sup>b</sup> Isolated yield.

the electron density of the substrate plays the key role in the photocatalytic oxidation of primary alcohols.

Furthermore, various secondary alcohols have been used to extend the scope of the 3D-RGO/ZnO photocatalytic method. As shown in Table 3, the secondary alcohol **3a** and **3b** bearing *m*- and *p*-methoxyl groups afford excellent yields of the products (Table 3, entries 1 and 2). When using  $-\text{H}$  instead, the efficiency was apparently not affected (Table 3, entry 3). However, electron-withdrawing groups obviously

**Table 3** Photocatalytic oxidation of secondary alcohols to ketones<sup>a</sup>



Entry	Substrate	Product	Yield/% <sup>b</sup>
1		<b>4a</b>	93
2		<b>4b</b>	89
3		<b>4c</b>	92
4		<b>4d</b>	87
5		<b>4e</b>	61
6		<b>4f</b>	95
7		<b>4g</b>	90
8		<b>4h</b>	86

<sup>a</sup> Reaction conditions: secondary alcohol **3** (1 mmol), 3D-RGO/ZnO catalyst (40 mg), DMF (5 mL), O<sub>2</sub> atmosphere, room temperature, 6 h.

<sup>b</sup> Isolated yield.

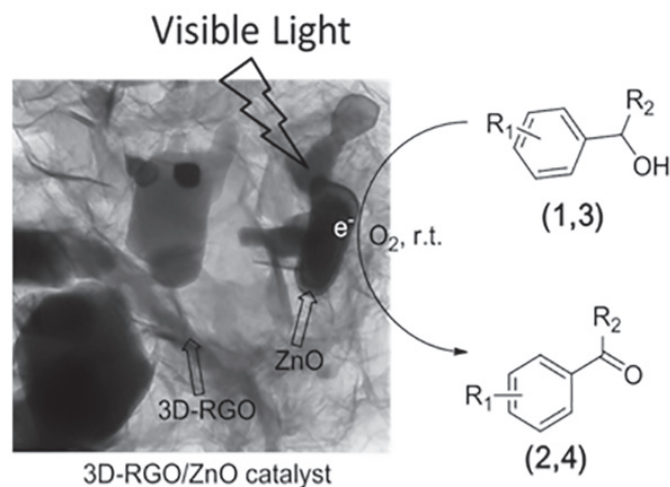


Fig. 2 Mechanism for the photocatalytic oxidation of alcohols.

influenced the oxidation reactions and moderate to low yields of target ketones were obtained (Table 3, entries 4 and 5). For diphenylmethanol **3f**, the reaction can proceed smoothly to furnish benzophenone **4f** in excellent yield (Table 3, entry 6). In addition, aryl cyclohexanol and cyclopentanol moieties could be smoothly oxidised to the corresponding products in good yields (Table 3, entries 7 and 8).

The photocatalytic process of the 3D-RGO/ZnO catalyst for the oxidation of alcohols is shown in Fig. 2. First, the electron was induced and transferred to the surface of nano ZnO under the irradiation of visible light. Then the photo-excited electron transfer to the substrate molecule was achieved through the 3D-RGO network. Finally, the corresponding aldehydes or ketones can be formed with the participation of oxygen.

## Conclusion

We prepared a 3D-RGO/ZnO photocatalyst through an *in situ* reduction of GO and the growth of nano ZnO particles. The 3D-RGO/ZnO displayed an enhanced photocatalytic effect towards commercial ZnO nanoparticles and can be applied to the oxidation of a broad series of benzyl alcohols including primary and secondary alcohols to the corresponding carbonyl compounds under the irradiation of visible light. A plausible photocatalytic mechanism referring to photo electron generation and transfer has been proposed. Further studies on the application of 3D-RGO/ZnO catalyst, such as photodegradation, are in progress.

This work was supported by Innovation and Promotion of Science-Technology Project of Zhejiang Province and Department of Education of Zhejiang Province of China under grant no. 20070546.

Received 6 August 2015; accepted 3 November 2015  
 Paper 1503529 doi: 10.3184/174751915X14476823418480  
 Published online: 1 December 2015

## References

- J. Jiao, L.X. Nguyen, D.R. Patterson and R.A. Flowers, *Org. Lett.*, 2007, **9**, 1323.
- S. Zhang, L. Xu and M.L. Trudell, *Synthesis*, 2005, **11**, 1757.
- E.J. Corey and J.W. Suggs, *Tetrahedron Lett.*, 1975, **16**, 2647.
- A. Shaabania, P. Mirzaeia, S. Naderia and D.G. Leeb, *Tetrahedron*, 2004, **60**, 11415.
- J.E. Steves and S.S. Stahl, *J. Am. Chem. Soc.*, 2013, **135**, 15742.
- M. Shibuya, M. Tomizawa, I. Suzuki and Y. Iwabuchi, *J. Am. Chem. Soc.*, 2006, **128**, 8412.
- M. Angelin, M. Hermansson, H. Dong and O. Ramström, *Eur. J. Org. Chem.*, 2006, **19**, 4323.
- K. Surendra, K.N. Srilakshmi, M.A. Reddy, Y.V.D. Nageswar and K.R. Rao, *J. Org. Chem.*, 2003, **68**, 2058.
- J.S. Yadav, B.V.S. Reddy, A.K. Basak and A.V. Narsaiah, *Tetrahedron*, 2004, **60**, 2131.
- N.S. Lewis and D.G. Nocera, *Proc. Natl. Acad. Sci. USA*, 2006, **103**, 15729.
- X.H. Li and M. Antonietti, *Chem. Soc. Rev.*, 2013, **42**, 6593.
- Z.J. Wang, S. Ghasimi, K. Landfester and K.A.I. Zhang, *Chem. Mater.*, 2015, **27**, 1921.
- Q. Xiao, S. Sarina, E. Jaatinen, J. Jia, D.P. Arnold, H. Liu and H. Zhu, *Green Chem.*, 2014, **16**, 4272.
- Q. Xiao, S. Sarina, A. Bo, J. Jia, H. Liu, D.P. Arnold, Y. Huang, H. Wu and H. Zhu, *ACS Catal.*, 2014, **4**, 1725.
- S. Sarina, H. Zhu, Q. Xiao, E. Jaatinen, J. Jia, Y. Huang, Z. Zheng and H. Wu, *Angew Chem. Int. Ed.*, 2014, **53**, 2935.
- S.H. Lee, J.H. Kim and C.B. Park, *Chem. Eur. J.*, 2013, **19**, 4392.
- C. Yu, G. Li, S. Kumar, K. Yang and R. Jin, *Adv. Mater.*, 2014, **26**, 892.
- J. Zhao, C. Chen and W. Ma, *Top Catal.*, 2005, **35**, 269.
- S. Higashimoto, N. Kitao, N. Yoshida, T. Sakura, M. Azuma, H. Ohue and Y.J. Sakata, *Catalysis*, 2009, **266**, 279.
- S. Choi, A.M. Berhane, A. Gentle, T. Cuong, M.R. Phillips and I. Aharonovich, *ACS Appl. Mater. Interfaces*, 2015, **7**, 5619.
- H. Arora, P.E. Malinowski, A. Chasin, D. Cheyns, S. Steudel, S. Schols and P. Heremans, *Appl. Phys. Lett.*, 2015, **106**, 143301.
- M.H. Dehghaniab and P. Mahdavia, *Desalination Water Treat.*, 2015, **54**, 3464.
- K. Chennakesavulua, M.M. Reddy, G.R. Reddy, A.M. Rabel, J. Brijitta, V. Vinita, T. Sasipraba and J. Sreeramulu, *J. Mol. Struct.*, 2015, **1091**, 49.
- M.V. Morales, E. Asedegbega-Nieto, A. Iglesias-Juez, I. Rodriguez-Ramos and A. Guerrero-Ruiz, *Chem. Sus. Chem.*, 2015, **8**, 2223.
- C.D. Zangmeister, *Chem. Mater.*, 2010, **22**, 5625.
- D. Li, M.B. Müller, S. Gilje, R.B. Kaner and G.G. Wallace, *Nat. Nanotech.*, 2008, **3**, 101.
- Y. Xu, K. Sheng, C. Li and G. Shi, *ACS Nano*, 2010, **4**, 4324.
- S. Stankovich, D.A. Dikin, D.H.B. Dommett, K.M. Kohlhaas, E.J. Zimney, E.A. Stach, P.D. Piner, S.T. Nguyen and R.S. Ruoff, *Nature*, 2006, **442**, 282.
- T. Ramanathan, A.A. Abdala, S. Stankovich, D.A. Dikin, M. Herrera-Alonso, R.D. Piner, D.H. Adamson, H.C. Schniepp, X. Chen, R.S. Ruoff, S.T. Nguyen, I.A. Aksay, R.K. Prudhomme and L.C. Brinson, *Nat. Nanotech.*, 2008, **3**, 327.
- M. Liu, J. Song, S. Shuang, C. Dong, J.D. Brennan and Y.A. Li, *ACS Nano*, 2014, **8**, 5564.
- M.F. Elkady, V. Strong, S. Dubin and R.B. Kaner, *Science*, 2012, **335**, 1326.
- V. Tjioa, J. Chua, S.S. Pramana, J. Wei, S.G. Mhaisalkar and N. Mathews, *ACS Appl. Mater. Interfaces*, 2012, **4**, 3447.
- H. Bi, X. Xie, K. Yin, Y. Zhou, S. Wan, L. He, F. Xu, F. Banhart, L. Sun and R.S. Ruoff, *Adv. Funct. Mater.*, 2012, **22**, 4421.
- C. Hu, Z. Mou, G. Lu, N. Chen, Z. Dong, M. Hu and L. Qu, *Phys. Chem. Chem. Phys.*, 2013, **5**, 13038.
- W. Gao, N. Singh, L. Song, Z. Liu, A.L.M. Reddy, L. Ci, R. Vajtai, Q. Zhang, B. Wei and P.M. Ajayan, *Nature Nanotech.*, 2011, **6**, 496.
- Y. Xu, K. Sheng, C. Li and G. Shi, *ACS Nano*, 2010, **4**, 4324.